Three-dimensionally printed navigational template: a promising guiding approach for lung biopsy

Haoran E[1#^], Jiafei Chen[1#], Weiyan Sun[1#], Yikai Zhang[2], Shengxiang Ren[3], Jingyun Shi[4], Yaofeng Wen[5], Chunxia Su[3], Jian Ni[3], Lei Zhang[1], Yayi He[3], Bin Chen[3], Roberto F. Casal[6], Fayez Kheir[7], Tsukasa Ishiwata[8], Jie Zhang[3], Deping Zhao[1], Chang Chen[1,9,10,11^]

[1]Department of Thoracic Surgery, Shanghai Pulmonary Hospital, School of Medicine, Tongji University, Shanghai, China; [2]School of Information Science and Technology, ShanghaiTech University, Shanghai, China; [3]Department of Medical Oncology, Shanghai Pulmonary Hospital, School of Medicine, Tongji University, Shanghai, China; [4]Department of Radiology, Shanghai Pulmonary Hospital, School of Medicine, Tongji University, Shanghai, China; [5]Lanhui Medical Technology Co., Ltd., Shanghai, China; [6]Department of Pulmonary Medicine, The University of Texas MD Anderson Cancer Center, Houston, TX, USA; [7]Division of Pulmonary and Critical Care Medicine, Department of Medicine, Massachusetts General Hospital, Harvard Medical School, Boston, MA, USA; [8]Division of Thoracic Surgery, Toronto General Hospital, University Health Network, Toronto, ON, Canada; [9]The International Science and Technology Cooperation Base for Development and Application of Key Technologies in Thoracic Surgery, Lanzhou, China; [10]Department of Thoracic Surgery, The First Hospital of Lanzhou University, Lanzhou, China; [11]The Province's Famous Expert Workstation, The First People's Hospital of Linhai, Taizhou, China

Contributions: (I) Conception and design: H E, J Chen, W Sun, C Chen; (II) Administrative support: C Chen, S Ren, D Zhao, J Zhang; (III) Provision of study materials or patients: H E, J Chen, W Sun, Y Wen, B Chen; (IV) Collection and assembly of data: W Sun, Y Zhang, J Ni, Y He, J Zhang; (V) Data analysis and interpretation: J Chen, L Zhang, J Shi, C Su, RF Casal, F Kheir, T Ishiwata, D Zhao; (VI) Manuscript writing: All authors; (VII) Final approval of manuscript: All authors.

[#]These authors contributed equally to this work.

Correspondence to: Jie Zhang, MD. Department of Medical Oncology, Shanghai Pulmonary Hospital, School of Medicine, Tongji University, 507 Zhengmin Road, Shanghai 200443, China. Email: zhangjie2172@163.com; Deping Zhao, MD; Chang Chen, MD, PhD. Department of Thoracic Surgery, Shanghai Pulmonary Hospital, School of Medicine, Tongji University, 507 Zhengmin Road, Shanghai 200443, China. Email: dpzhao@tongji.edu.cn; chenthoracic@163.com.

Background: Percutaneous transthoracic lung biopsy is customarily conducted under computed tomography (CT) guidance, which primarily depends on the conductors' experience and inevitably contributes to long procedural duration and radiation exposure. Novel technique facilitating lung biopsy is currently demanded.

Methods: Based on the reconstructed anatomical information of CT scans, a three-dimensionally printed navigational template was customized to guide fine-needle aspiration (FNA). The needle insertion site and angle could be indicated by the template after proper placement according to the reference landmarks. From June 2020 to August 2020, patients with peripheral indeterminate lung lesions ≥30 mm in diameter were enrolled in a pilot trial. Cases were considered successful when the virtual line indicated by the template in the first CT scan was pointing at the target, and the rate of success was recorded. The insertion deviation, procedural duration, radiation exposure, biopsy-related complications, and diagnostic yield were documented as well.

Results: A total of 20 patients consented to participate, and 2 withdrew. The remaining 18 participants consisting of 11 men and 7 women with a median age of 63 [inter-quartile range (IQR), 50–68] years and a median body mass index (BMI) of 23.5 (IQR, 20.8–25.8) kg/m^2 received template-guided FNA. The median nodule size of the patients was 41.2 (IQR, 36.2–51.9) mm and 17 lesions were successfully targeted (success rate, 94.4%). One lesion was not reached through the designed trajectory due to an unpredictable alteration of the lesion's location resulting from pleural effusion. The median deviation between the actual position

^ ORCID: Haoran E, 0000-0002-9160-7646; Chang Chen, 0000-0002-9981-3110.

of the needle tip and the designed route was 9.4 (IQR, 6.8–11.7) mm. The median procedural duration was 10.7 (IQR, 9.7–11.8) min, and the median radiation exposure was 220.9 (IQR, 198.6–249.5) mGy×cm. No major biopsy-related complication was encountered. Definitive diagnosis of malignancy was reached in 13 of the 17 (76.5%) participants.

Conclusions: The feasibility and safety of navigational template-guided FNA were preliminarily validated in lung biopsy cohort. Nonetheless, patients with pleural effusion were not recommended to undergo FNA guided by such technique.

Trial Registration: This study was registered with ClinicalTrials.gov (identifier: NCT03325907).

Keywords: Lung biopsy; three-dimensional printing (3D printing); computed tomography (CT); fine-needle aspiration (FNA)

Introduction

Lung biopsy is a routinely performed procedure in clinical practice, which is of fundamental importance in establishing the diagnosis of lung lesions and patient management (1). For peripherally localized lung lesions, the two most popular biopsy techniques involve computed tomography (CT)-guided percutaneous biopsy and advanced bronchoscopy, with CT-guided percutaneous transthoracic fine-needle aspiration (FNA) serving as a major strategy for diagnosis (2), with diagnostic accuracy ranging from 76.0% to 93.4% (3-12). Despite the high diagnostic efficacy, several drawbacks of this kind of biopsy procedure still cannot be avoided. Firstly, the puncture angle of the biopsy needle is manually determined with the guidance of CT scanning, which largely depends on the experience of the operators and has a long procedural duration. Furthermore, CT scanning inevitably leads to radiation exposure. Moreover, repeated adjustments of the biopsy needle before accurate insertion are usually required, which also increases the procedure time and the radiation dose. Repeated insertion attempts also contribute to a high rate of pneumothorax, pulmonary hemorrhage, and other biopsy-related complications (13-20).

Three-dimensional (3D) printing has been exploited in a wide variety of medical fields (21), showing tremendous potential in preoperative planning, implant design, and training. Based on the explicit strength of 3D printing in customized reconstruction of radiological images, the concept of utilizing such technique in surgical navigation was afterwards brought up. Kunz *et al.* reported an individualized drilling templates designed for hip resurfacing surgery, demonstrating equivalent accuracy to conventional CT assisted approach (22). Similar results were also obtained in template-guided mandibular defect repair surgery as reported by Liu *et al.* (23). Hereafter, numerous researchers further evaluated the availability of navigational template used for surgical guidance in maxillofacial and orthopedic operations (24-26). Likewise, our team developed a navigational template to guide the preoperative localization of small lung nodules. The efficacy and safety of template-guided nodule localization have been validated in series of clinical trials (27-29). As the demand for accuracy is higher in FNA than in preoperative nodule localization, whether this kind of template is applicable for FNA remains unknown. We further modified our prior study's design (27) and developed a navigational template applicable for FNA. This study was conducted to investigate the feasibility of template-guided FNA for peripheral lung lesions. Furthermore, we present the following article in accordance with the TREND reporting checklist (available at https://tlcr.amegroups.com/article/view/10.21037/tlcr-22-172/rc).

Methods

Study design

This study was a single-center, prospective pilot trial for 3D printed navigational template guided lung biopsy, which was conducted in accordance with the Declaration of Helsinki (as revised in 2013). From June 2020 to August 2020, patients scheduled for percutaneous transthoracic FNA were recruited. Written informed consent was obtained
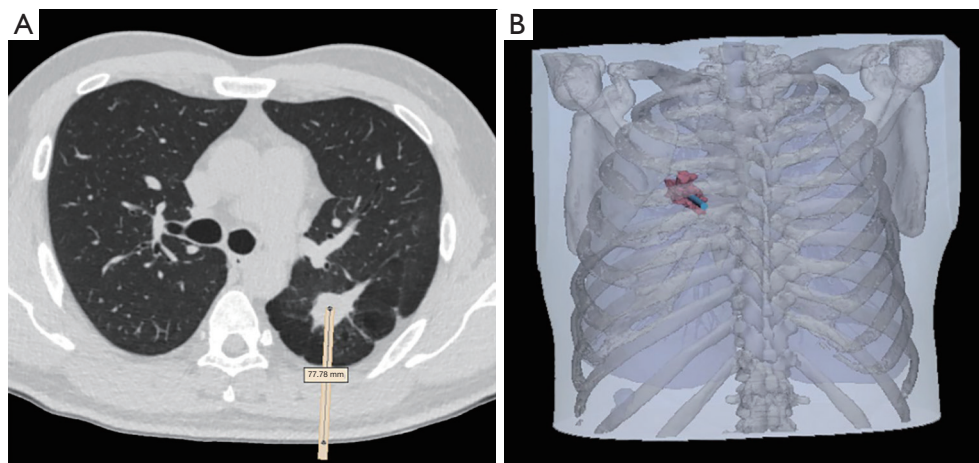
Figure 1 Insertion route design and reconstruction of the CT images. The insertion route was designed by the referring pulmonologist based on the CT images (A). The whole thorax consisting of the target lesion (red part), insertion route (blue part), thoracic contour surface (purple part), and bony cage (grey part) was reconstructed and shown from the back (B) view. CT, computed tomography.

before patient enrollment. Both the pulmonologists (SR, CS, JN, YH, BC and JZ) and the radiologist (JS) reviewed the CT images to select the eligible participants. The main inclusion criterion was peripheral lung lesions [as classified by Baaklini *et al.* (30)] with a long-axis diameter ≥30 mm scheduled for lung biopsy. Lesions shielded by the scapula or situated close to the diaphragm (center of the lesion within 3 cm of the diaphragm) or those with contraindications for lung biopsy were excluded. Besides, the study was approved by the Institutional Review Board of Shanghai Pulmonary Hospital (No. K17-155) and was registered with ClinicalTrials.gov (identifier: NCT03325907).

Procedures

Template design and printing

Participants' CT scan images (non-contrast, slice thickness 1.5 mm, obtained for clinical purposes) were acquired from the Picture Archiving and Communication Systems, and a 3D thorax model was reconstructed using Mimics Research 20.0 and Magics 21.0 (Materialise NV, Leuven, Belgium). The insertion route was designed based on the CT images and the thorax model following the principle of choosing the shortest route and avoiding any major anatomical structures (*Figure 1*). The prominent anatomical landmarks of the thoracic bony cage were subsequently selected and projected, and 2 marks recognizing the sternal end of the clavicle and the costal arch were also included in the design (Figure S1). The navigational template was then delineated

in accordance with the thoracic contour (*Figure 2*). Finally, the whole template was printed using stereolithography from photopolymer material (Figure S1). It took approximately 1 hour to design the model and 5–6 hours to print it. The cost per person for developing the template was $75–90. Detailed design and printing procedure was demonstrated in our previous research (27).

Navigational template-guided lung biopsy

Percutaneous transthoracic FNA was performed in the radiology department (*Figure 3*). The participant's decubitus position was decided according to the location of the puncture site. The template was placed with the guidance of the anatomical landmarks and was secured to the patient using medical tape. Then, an initial CT scan was performed to evaluate the feasibility of template-guided biopsy. A virtual line was drawn on the CT images through the insertion point to simulate the insertion path of the biopsy needle. If the virtual line was targeted at the lesion, it was considered appropriate to conduct FNA and recorded as a successful case. The success rate of navigational template-guided biopsy would be ultimately analyzed. Next, sterilization and local anesthesia with 2% lidocaine were administered. The biopsy needle (ChibaSono, Germany; 22-gauge, 10 cm length) was inserted to the predetermined depth following deep inhalation of the participant, and a second CT scan was subsequently performed, based on which 3D deviations were calculated. If the virtual line did not point to the targeted lesion, the template-guided FNA
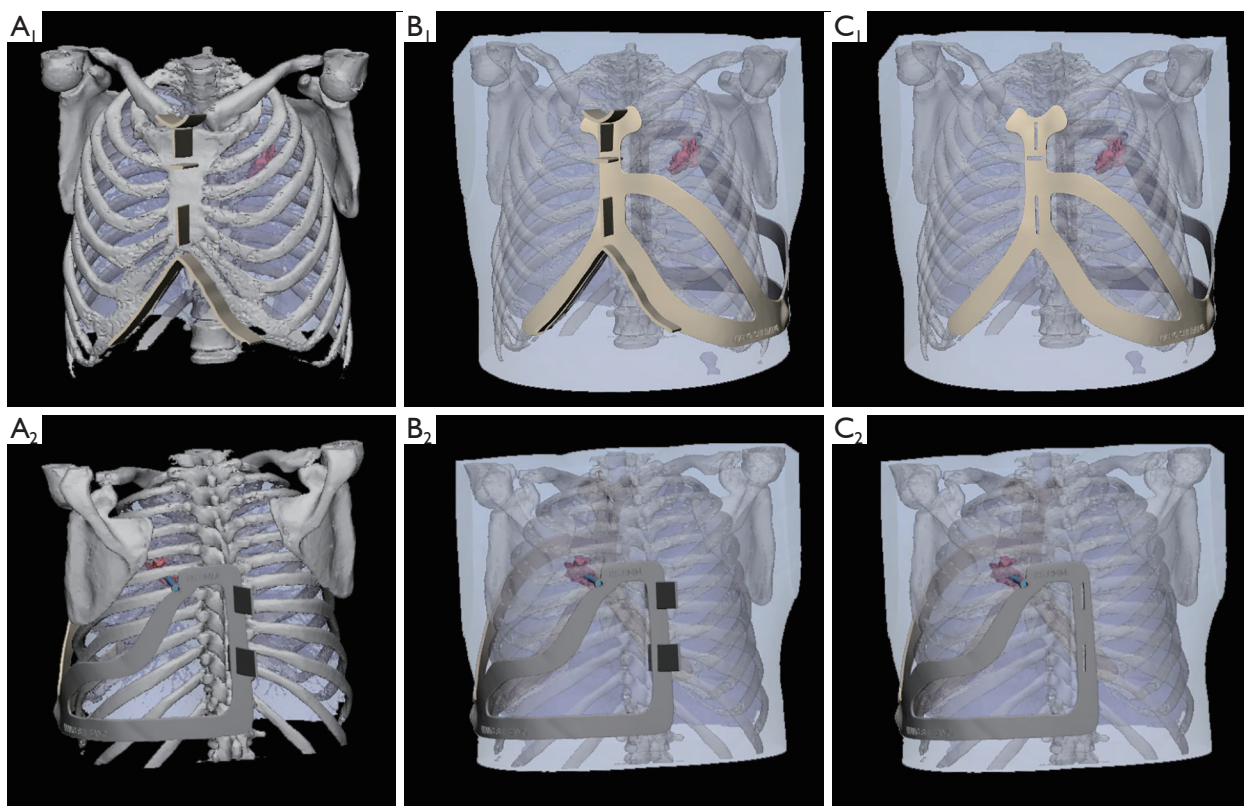
396

E et al. Navigational template-guided lung biopsy

Figure 2 Navigational template design process. Prominent anatomical landmarks guiding accurate localization of the template were selected and horizontally projected (A). The navigational template was delineated according to the contour of the body surface encompassing the anatomical landmarks and insertion route (B). The overlapping part of the navigational template and projection parts of the anatomical landmarks were eliminated by means of a Boolean algorithm (C).

was recorded as a failure, and the participant was subjected to a traditional CT-guided FNA.

Subsequently, percutaneous transthoracic FNA was implemented. The acquired cells were used for cytological examination. Moreover, according to the pulmonologists' instructions, some participants also received a coaxial needle biopsy (CNB) for histological examination (biopsy needle, GALLINI S. R. L., Italy, 18-gauge, 16 cm length). The CNB could only be conducted after FNA. Once the biopsy was finished, the needle was retrieved and the puncture site was covered with gauze. After all these procedures, a final CT scan was performed to evaluate biopsy-related complications.

Evaluation parameters concerning the biopsy procedure

The distance between the actual position of the needle tip and the exact center of the target lesion, which was also

the end of the designed route, was defined as the insertion deviation, and the coronal (CD), axial (AD), and sagittal deviations (SD) were measured separately (Figure S2). The total deviation (TD) was calculated as follows {Eq. [1]}:

$$TD = \sqrt{CD^2 + AD^2 + SD^2} \qquad [1]$$

The deviation direction was also recorded, among which the negative values for the CD, AD, or SD indicated that the biopsy needle deviated laterally, posteriorly, or caudally, respectively.

The procedural duration was measured from the first CT scan to the last one. The cumulative radiation dose was recorded by the CT scanner (SIEMENS 64-slice spiral CT, SOMATOM, Definition AS, Siemens Co., Ltd.). Biopsy-related complications were classified as minor or major complications according to the Society of Interventional Radiology (SIR) Guidelines (31). For those
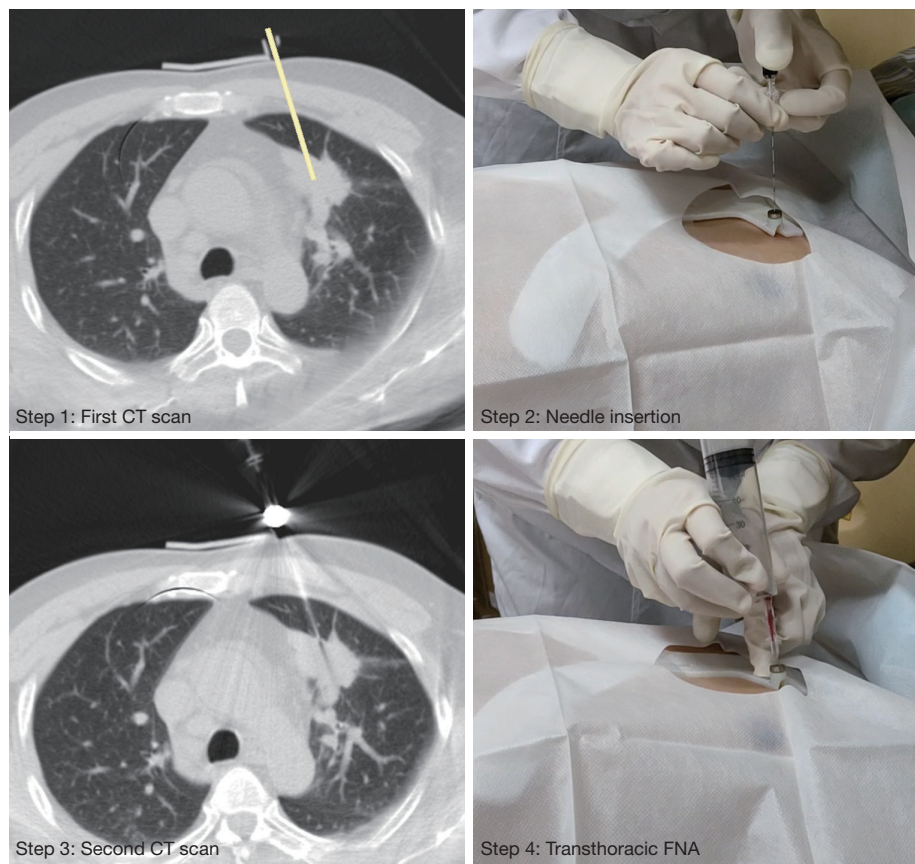
Figure 3 Template-guided biopsy procedure. After the placement of the template, the first CT scan was performed to evaluate the appropriateness of needle insertion, and an imaginary yellow line was drawn through the protrusion of the template (step 1). After the confirmation CT scan, sterilization and local anesthesia were subsequently administered. The biopsy needle was then inserted to the preset depth (step 2), and another CT scan was performed to calculate the insertion deviation (step 3), after which the core of the biopsy needle was drawn out and the needle was connected to a 50 mL syringe. The force inside the syringe created a vacuum, which allowed for the tumor cells to be suctioned out through the needle (step 4). CT, computed tomography; FNA, fine-needle aspiration.

who underwent CNB at the same time, the aforementioned three parameters concerning FNA only were recorded. In addition, the cytological results of the FNA were classified into categories including malignancy, suspicious for malignancy, specific benign and nondiagnostic findings.

Statistical analysis

The participants' demographic information and clinicopathological features were collected. The continuous variables were expressed as median with 25th-75th percentiles [inter-quartile range (IQR)], and were analyzed using an independent *t*-test. The categorical variables were expressed as number with percentage and were analyzed using Pearson's chi-squared test. A P value of less than 0.05 was considered as

a significant difference, and all the data were analyzed using SPSS (version 26.0; IBM SPSS Inc., Armonk, NY, USA).

Results

Between June 2020 and August 2020, 22 patients scheduled for percutaneous transthoracic FNA were enrolled during the pre-selection, and 20 patients consented to participate. Among them, 2 patients dropped out of the study due to temporary rescheduling for ultrasound (US)-guided percutaneous biopsy and a temporary change of the insertion route made by the corresponding pulmonologist. Altogether, 18 participants [median age, 63 (IQR, 50–68) years] consisting of 11 men and 7 women, all of whom were Asians, underwent template-guided FNA.

398

E et al. Navigational template-guided lung biopsy

Table 1 Clinical characteristics of the participants undergoing template-guided FNA

Parameters	N
Sex, % male	61.1 (11/18)
Age, years	63 [50–68][a]
Race, n (%)	
Asians	18 (100.0)
BMI, kg/m^2	23.5 [20.8–25.8][a]
Nodule size, mm	41.2 [36.2–51.9][a]
Distance between the lesion and pleura, mm	2.2 [0.0–11.3][a]
Nodule location, n (%)	
UL + ML	14 (77.8)
LL	4 (22.2)
Biopsy type, n (%)	
FNA alone	10 (55.6)
FNA + CNB	8 (44.4)
Decubitus position, % supine	55.6 (10/18)
Length of the insertion route, mm	80.2 [70.4–85.8][a]

[a], age, BMI, nodule size, distance between the lesion and pleura, and length of the insertion route were expressed as median [IQR]. FNA, fine-needle aspiration; BMI, body mass index; UL, upper lobe; ML, middle lobe; LL, lower lobe; CNB, coaxial needle biopsy; IQR, inter-quartile range.

Table 2 Characteristics related to the template-guided FNA procedure

Parameters	N
Successfully targeted events, n (%)	17 (94.4)
Insertion deviation value, mm	
Coronal	2.1 [0.7–5.8][a]
Axial	4.4 [1.9–7.5][a]
Sagittal	4.3 [1.4–8.5][a]
Total	9.4 [6.8–11.7][a]
Procedural duration, min	10.7 [9.7–11.8][a]
DLP, mGy×cm	220.9 [198.6–249.5][a]
Pneumothorax, n (%)	2 (11.8)[b]
Hemorrhage, n (%)	3 (17.6)[b]
Cytological examination results, n (%)	
Malignancy	13 (76.5)
Primary lung	11 (64.7)
Adenocarcinoma	6 (35.3)
Non-small cell carcinoma	5 (29.4)
Malignancy, poorly differentiated	2 (11.8)
Suspicious for malignancy	1 (5.9)
Inadequate samples	3 (17.6)

[a], insertion deviation, procedural duration, and DLP were expressed as median [IQR]; [b], no participant needed further intervention. FNA, fine-needle aspiration; DLP, dose-length product; IQR, inter-quartile range.

The participants' baseline information, the characteristics of the lesions, and the biopsy procedure are summarized in *Table 1*. The median body mass index (BMI) value was 23.5 (IQR, 20.8–25.8) kg/m^2. The median diameter of the lesions was 41.2 (IQR, 36.2–51.9) mm. The median distance between the outer edge of the lesion to the pleural surface was 2.2 (range, 0.0–16.6) mm. Most of the lesions were located in the upper and middle lobes (14/18, 77.8%). All the participants received FNA, and 8 participants also underwent CNB. Ten participants (10/18, 55.6%) received a biopsy in the supine position, and the remaining were in the lateral position. The median length of the designed needle insertion route was 80.2 (IQR, 70.4–85.8) mm.

The template-guided FNA procedure was successfully carried out in 17 participants (17/18, 94.4%) and all these participants' needle insertion CT images are shown in Figures S3,S4. The biopsy needle did not reach 1 lesion through the predesigned route due to an unpredictable alteration of the lesion's location. In this participant, the

pre-biopsy CT image revealed a pleural effusion which measured 31.4 mm in the long-axis diameter in the right thoracic cavity. The insertion route was initially designed through the right eighth intercostal space. After the participant was placed in a lateral decubitus position, the fluid that accumulated in the bottom of the cavity redistributed, resulting in the alteration of the relative position between the thoracic cage and the lesion. Thus, the lesion could not be targeted through the predesigned intercostal space (Figure S5). The participant was then arranged to undergo a CT-guided approach.

The characteristics related to the procedure of the 17 successful cases are listed in *Table 2*. The median deviations in the coronal, axial, and sagittal directions were 2.1, 4.4, and 4.3 mm, respectively. The median TD of the biopsy needle was 9.4 (IQR, 6.8–11.7) mm. After taking the
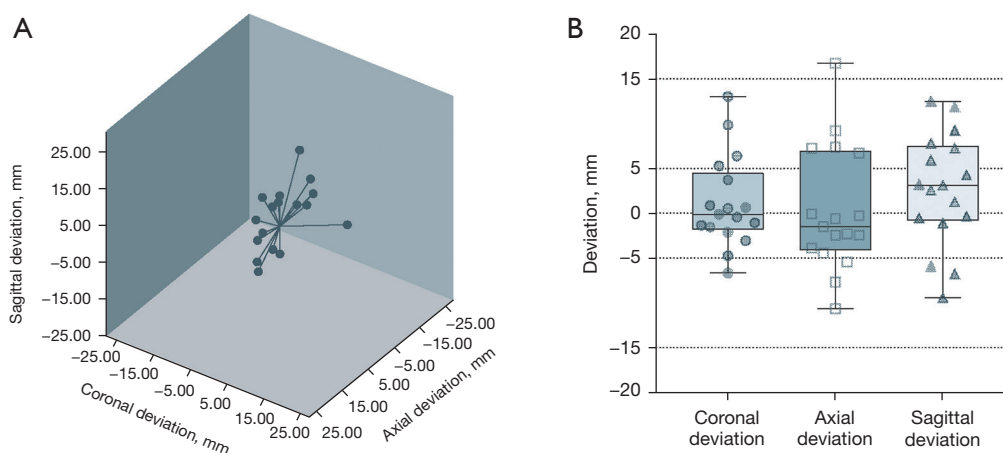
Figure 4 Deviations of template-guided FNA. The deviations of template-guided FNA were demonstrated three-dimensionally (A). Positive values for CD, AD, or SD indicated that the biopsy needle deviated medially, anteriorly, or cranially, respectively. The deviations in each dimension were further compared (B). The horizontal line in each box indicates the median, while the top and bottom borders of each box indicate the 75th and 25th percentiles, respectively. The ends of the whiskers above and below each box indicate the minimum and maximum values. FNA, fine-needle aspiration; CD, coronal deviation; AD, axial deviation; SD, sagittal deviation.

deviation direction into account, most of the biopsy needles deviated medially, anteriorly, and cranially (*Figure 4*). The median procedural duration of the FNA was 10.7 (IQR, 9.7–11.8) min, and the median radiation exposure was 220.9 (IQR, 198.6–249.5) mGy×cm. FNA-related complications were encountered in 5 cases (5/17, 29.4%), including 2 cases of asymptomatic pneumothorax and 3 cases of pulmonary hemorrhage. The maximum degree of collapse of the lung post FNA was 5%, and the maximum diameter of the biopsy-related hematoma was 5.1 mm, both of which were evaluated based on the CT images acquired post biopsy. None of these participants needed further intervention. No major complication was encountered during the procedure. The FNA-acquired specimens were diagnosed positive for malignancy in 13 lesions, including 11 lesions diagnosed as primary lung tumor and 2 lesions as poorly differentiated. Suspicious malignant cells were recognized in 1 case, who subsequently undertook bronchoscopic biopsy and finally obtained a malignant diagnosis, while another 3 samples were evaluated nondiagnostic, with 2 patients proved malignant through CNB and 1 patient still in follow-up. The specific clinical characteristics and clinicopathological information of these 17 cases are summarized separately in Tables S1,S2.

Discussion

CT-guided percutaneous transthoracic FNA is a well-

established method for determining the cytopathological diagnosis of peripheral lung lesions. The diagnostic yield of this procedure is high, with an average sensitivity and specificity of 82.0–98.4% and 96.2–100.0%, respectively (3-6,8,9). Nonetheless, since such procedure was manually conducted, repeated adjustments constantly occur, which inevitably complicates the process, resulting in prolonged duration, increased radiation exposure, and an elevated complication rate. Furthermore, such procedure is typically performed by interventional radiologist and not widely applicable to interventional pulmonologists or thoracic surgeons. To simplify the transthoracic FNA procedure and provide the operators from different specialties safe and stable guiding method, we reported a navigational template developed using 3D printing technology. This navigational template is applicable for transthoracic FNA and was modified based on our prior study's design (27) to meet a higher demand for accuracy. With the guidance of this modified navigational template, the procedure was successfully carried out in 17 out of 18 participants (94.4%) who underwent FNA. The feasibility of template-guided FNA was preliminarily validated in this prospective pilot study. Besides, compared with previously reported results, the radiation exposure the patients received was decreased (32,33), which further illustrated the safety of template-guided procedure.

As elucidated in previous studies (27-29), the skeletal features of patients serve as accurate and stable reference

400

E et al. Navigational template-guided lung biopsy

landmarks when placing the navigational template. The routinely chosen skeletal landmarks include the upper edge of the sternum, the Louis angle, the substernal angle, the midline of the sternum, and the posterior midline correlated to the spinous process. The feasibility of selecting these features as reference landmarks to develop a template for guiding the preoperative localization of pulmonary nodules was validated. Nonetheless, since these skeletal features lay approximately in the same sagittal plane, the overall accuracy of template-guided preoperative localization was limited as reported in our previous study (27), with a maximum deviation of over 20 mm. Compared with nodule localization, the transthoracic FNA biopsy procedure has a higher demand for needle insertion accuracy in order to obtain sufficient specimens for cytopathological diagnoses. To meet this demand, additional elements recognizing the sternal end of the clavicle and the costal arch were added to the design of the template for reconfirming the position in the coronal plane (Figure S6). The final results showed that a maximum deviation of 15.2 mm (Case 12) was achieved in this pilot study [TD, preoperative localization (29) *vs.* FNA, 8.7±6.9 *vs.* 9.3±3.1 mm].

Another factor affecting placement precision is respiratory movement. The existence of such movements results in the constant deformation of the thorax contour, which substantially influences the template placement procedure. Hence, a method for controlling the respiratory phase to minimize respiratory deviation is needed. Since the CT scan images used for developing the template were taken after a deep inhalation, the process of placing the template and inserting the needle were only conducted after a deep inhalation and breath-hold. With this method, the respiratory phase, when the biopsy was conducted, approached that of when the initial CT scanning was performed.

With the guidance of the modified navigational template and the assistance of the respiratory control method, transthoracic FNA was successfully carried out in 17 participants. One case failed, which served as a reference candidate for selecting suitable patients. The failed case resulted from an unpredictable alteration of the tumor's location due to pleural effusion. The lung tissue distortion contributed to the movement of the fluid accumulated in the thoracic cavity when the participant adopted different decubitus positions. Hence, the aforementioned prominent features contributed to the unpredictable alteration of the lesion's position when the biopsy was conducted in a lateral position. It also indicates that patients with newly emerged pleural effusion are not eligible to undergo FNA using

navigational template designed by the previous CT images. Some researchers have already reported using augmented reality (AR)-based calibration method to optically navigate otorhinolaryngological surgeries (34,35), such notion of movement calibration might also have the potential of calibrating the deviations of the pulmonary lesions resulted from newly emerged pleural effusion or atelectasis. Besides, since the diameters of lesions of the patients in this study were relatively large, utilizing such template in small nodule biopsy was still challenging. Electromagnetic navigation bronchoscopy is a newly-developed modality in lung biopsy, with an impressive accuracy in peripheral pulmonary lesions diagnosis (36,37). Since the application of such modality has been reported by many researchers and also feasible in our institution, further study utilizing 3D printing technology in combination with electromagnetic navigation method might harbor the potential of improving the accuracy of lung biopsy.

There are several limitations of this study. First, the sample size of this pilot study was relatively small. In addition, no comparison between this novel technique and the conventional CT method in terms of the procedural duration, radiation dose, and biopsy-related complication rate was performed. The comparison between these two methods in specific diagnosis or histological subtype evaluation was also missing. Hence, a randomized controlled trial evaluating these two methods is actively recruiting (ClinicalTrials.gov identifier: NCT04775901). Second, the median BMI of the participants in this study was 23.5 kg/m^2. Whether this modified navigational template is applicable for obese patients still needs evaluating. Lastly, the needle insertion accuracy of the 3D navigational template was preliminarily evaluated in this study, but data concerning the diagnostic efficacy of this technique is still lacking. Hence, a more comprehensive assessment and follow-up plan is warranted to further analyze the diagnostic accuracy.

In conclusion, the feasibility of 3D printed navigational template-guided FNA has been validated. Nonetheless, since the diagnostic accuracy of template-guided lung biopsy was not evaluated, further studies should be designed to confirm whether a noninferior result regarding diagnostic yield can be achieved compared with the CT-guided modality.

Acknowledgments

Footnote

Reporting Checklist: The authors have completed the TREND reporting checklist. Available at https://tlcr.amegroups.com/article/view/10.21037/tlcr-22-172/rc

Data Sharing Statement: Available at https://tlcr.amegroups.com/article/view/10.21037/tlcr-22-172/dss

Conflicts of Interest: All authors have completed the ICMJE uniform disclosure form (available at https://tlcr.amegroups.com/article/view/10.21037/tlcr-22-172/coif). YW is a current employee of Lanhui Medical Technology Co., Ltd. The other authors have no conflicts of interest to declare.

Ethical Statement: The authors are accountable for all aspects of the work in ensuring that questions related to the accuracy or integrity of any part of the work are appropriately investigated and resolved. The study was conducted in accordance with the Declaration of Helsinki (as revised in 2013). The study was approved by the Institutional Review Board of Shanghai Pulmonary Hospital (No. K17-155) and written informed consent was obtained before patient enrollment.

References

1. Manhire A, Charig M, Clelland C, et al. Guidelines for radiologically guided lung biopsy. Thorax 2003;58:920-36.
2. Rivera MP, Mehta AC, Wahidi MM. Establishing the diagnosis of lung cancer: Diagnosis and management of lung cancer, 3rd ed: American College of Chest Physicians evidence-based clinical practice guidelines. Chest 2013;143:e142S-65S.
3. García Río F, Díaz Lobato S, Pino JM, et al. Value of CT-guided fine needle aspiration in solitary pulmonary nodules with negative fiberoptic bronchoscopy. Acta Radiol 1994;35:478-80.
4. Böcking A, Klose KC, Kyll HJ, et al. Cytologic versus histologic evaluation of needle biopsy of the lung, hilum and mediastinum. Sensitivity, specificity and typing accuracy. Acta Cytol 1995;39:463-71.
5. Li H, Boiselle PM, Shepard JO, et al. Diagnostic accuracy and safety of CT-guided percutaneous needle aspiration biopsy of the lung: comparison of small and large pulmonary nodules. AJR Am J Roentgenol 1996;167:105-9.
6. Santambrogio L, Nosotti M, Bellaviti N, et al. CT-guided fine-needle aspiration cytology of solitary pulmonary nodules: a prospective, randomized study of immediate cytologic evaluation. Chest 1997;112:423-5.
7. Larscheid RC, Thorpe PE, Scott WJ. Percutaneous transthoracic needle aspiration biopsy: a comprehensive review of its current role in the diagnosis and treatment of lung tumors. Chest 1998;114:704-9.
8. Arslan S, Yilmaz A, Bayramgürler B, et al. CT-guided transthoracic fine needle aspiration of pulmonary lesions: accuracy and complications in 294 patients. Med Sci Monit 2002;8:CR493-7.
9. Wallace MJ, Krishnamurthy S, Broemeling LD, et al. CT-guided percutaneous fine-needle aspiration biopsy of small (< or =1-cm) pulmonary lesions. Radiology 2002;225:823-8.
10. Geraghty PR, Kee ST, McFarlane G, et al. CT-guided transthoracic needle aspiration biopsy of pulmonary nodules: needle size and pneumothorax rate. Radiology 2003;229:475-81.
11. Laspas F, Roussakis A, Efthimiadou R, et al. Percutaneous CT-guided fine-needle aspiration of pulmonary lesions: Results and complications in 409 patients. J Med Imaging Radiat Oncol 2008;52:458-62.
12. Choi SH, Chae EJ, Kim JE, et al. Percutaneous CT-guided aspiration and core biopsy of pulmonary nodules

402

E et al. Navigational template-guided lung biopsy

smaller than 1 cm: analysis of outcomes of 305 procedures from a tertiary referral center. AJR Am J Roentgenol 2013;201:964-70.

13. Laurent F, Latrabe V, Vergier B, et al. Percutaneous CT-guided biopsy of the lung: comparison between aspiration and automated cutting needles using a coaxial technique. Cardiovasc Intervent Radiol 2000;23:266-72.

14. Noh TJ, Lee CH, Kang YA, et al. Chest computed tomography (CT) immediately after CT-guided transthoracic needle aspiration biopsy as a predictor of overt pneumothorax. Korean J Intern Med 2009;24:343-9.

15. Priola AM, Priola SM, Cataldi A, et al. Diagnostic accuracy and complication rate of CT-guided fine needle aspiration biopsy of lung lesions: a study based on the experience of the cytopathologist. Acta Radiol 2010;51:527-33.

16. Hiraki T, Mimura H, Gobara H, et al. Incidence of and risk factors for pneumothorax and chest tube placement after CT fluoroscopy-guided percutaneous lung biopsy: retrospective analysis of the procedures conducted over a 9-year period. AJR Am J Roentgenol 2010;194:809-14.

17. Wiener RS, Schwartz LM, Woloshin S, et al. Population-based risk for complications after transthoracic needle lung biopsy of a pulmonary nodule: an analysis of discharge records. Ann Intern Med 2011;155:137-44.

18. Kuban JD, Tam AL, Huang SY, et al. The Effect of Needle Gauge on the Risk of Pneumothorax and Chest Tube Placement After Percutaneous Computed Tomographic (CT)-Guided Lung Biopsy. Cardiovasc Intervent Radiol 2015;38:1595-602.

19. Anzidei M, Sacconi B, Fraioli F, et al. Development of a prediction model and risk score for procedure-related complications in patients undergoing percutaneous computed tomography-guided lung biopsy. Eur J Cardiothorac Surg 2015;48:e1-6.

20. Heerink WJ, de Bock GH, de Jonge GJ, et al. Complication rates of CT-guided transthoracic lung biopsy: meta-analysis. Eur Radiol 2017;27:138-48.

21. Martelli N, Serrano C, van den Brink H, et al. Advantages and disadvantages of 3-dimensional printing in surgery: A systematic review. Surgery 2016;159:1485-500.

22. Kunz M, Rudan JF, Xenoyannis GL, et al. Computer-assisted hip resurfacing using individualized drill templates. J Arthroplasty 2010;25:600-6.

23. Liu YF, Xu LW, Zhu HY, et al. Technical procedures for template-guided surgery for mandibular reconstruction based on digital design and manufacturing. Biomed Eng Online 2014;13:63.

24. Schweizer A, Fürnstahl P, Nagy L. Three-dimensional correction of distal radius intra-articular malunions using patient-specific drill guides. J Hand Surg Am 2013;38:2339-47.

25. Liang J, Zhao Y, Gao X, et al. Design of custom-made navigational template of femoral head and pilot research in total hip resurfacing arthroplasty. BMC Surg 2020;20:144.

26. Li Z, Xu D, Li F, et al. Design and application of a novel patient-specific 3D printed drill navigational guiding template in percutaneous thoracolumbar pedicle screw fixation: A cadaveric study. J Clin Neurosci 2020;73:294-8.

27. Zhang L, Li M, Li Z, et al. Three-dimensional printing of navigational template in localization of pulmonary nodule: A pilot study. J Thorac Cardiovasc Surg 2017;154:2113-9.e7.

28. Sun W, Zhang L, Wang L, et al. Three-Dimensionally Printed Template for Percutaneous Localization of Multiple Lung Nodules. Ann Thorac Surg 2019;108:883-8.

29. Zhang L, Wang L, Kadeer X, et al. Accuracy of a 3-Dimensionally Printed Navigational Template for Localizing Small Pulmonary Nodules: A Noninferiority Randomized Clinical Trial. JAMA Surg 2019;154:295-303.

30. Baaklini WA, Reinoso MA, Gorin AB, et al. Diagnostic yield of fiberoptic bronchoscopy in evaluating solitary pulmonary nodules. Chest 2000;117:1049-54.

31. Sacks D, McClenny TE, Cardella JF, et al. Society of Interventional Radiology clinical practice guidelines. J Vasc Interv Radiol 2003;14:S199-202.

32. Michel M, Jacob S, Roger G, et al. Eye lens radiation exposure and repeated head CT scans: A problem to keep in mind. Eur J Radiol 2012;81:1896-900.

33. Fu YF, Li GC, Xu QS, et al. Computed tomography-guided lung biopsy: a randomized controlled trial of low-dose versus standard-dose protocol. Eur Radiol 2020;30:1584-92.

34. Sun Q, Mai Y, Yang R, et al. Fast and accurate online calibration of optical see-through head-mounted display for AR-based surgical navigation using Microsoft HoloLens. Int J Comput Assist Radiol Surg 2020;15:1907-19.

35. Chen X, Xu L, Wang Y, et al. Development of a surgical navigation system based on augmented reality using an optical see-through head-mounted display. J Biomed Inform 2015;55:124-31.

36. Folch EE, Pritchett MA, Nead MA, et al. Electromagnetic Navigation Bronchoscopy for Peripheral Pulmonary Lesions: One-Year Results of the Prospective, Multicenter

NAVIGATE Study. J Thorac Oncol 2019;14:445-58.

37. Ishiwata T, Ujiie H, Gregor A, et al. Pilot study using virtual 4-D tracking electromagnetic navigation bronchoscopy in the diagnosis of pulmonary nodules:

a single center prospective study. J Thorac Dis 2021;13:2885-95.

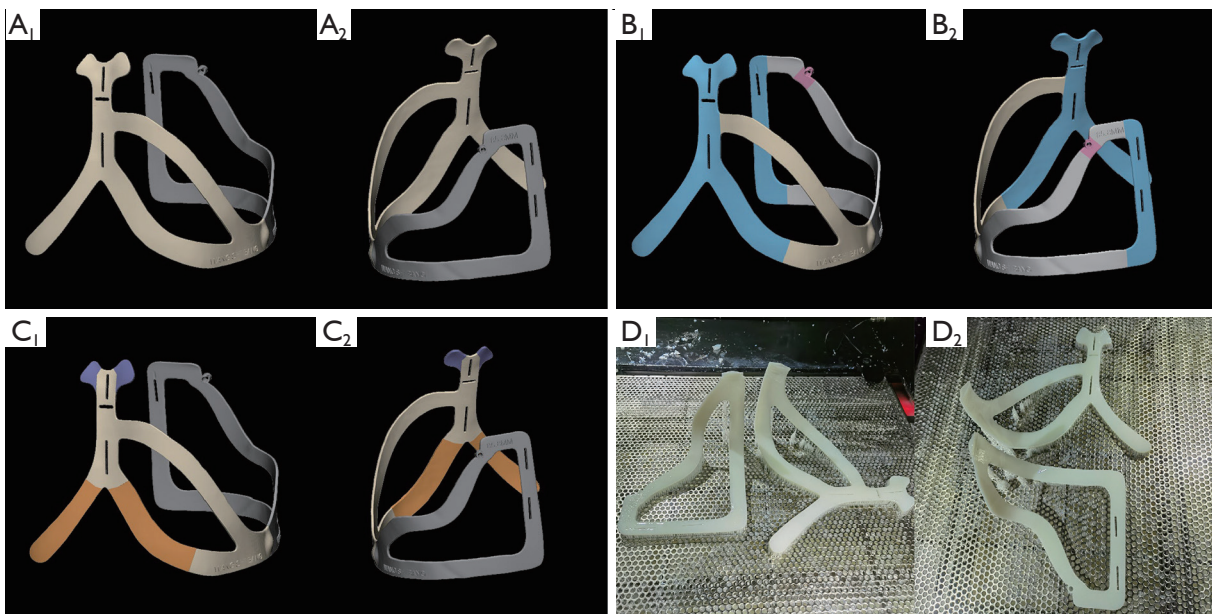(English Language Editor: C. Betlazar-Maseh)

Figure S1 Printing of the navigational template. The model of the whole template is shown from the front view (A1) and back view (A2). The navigational template was further divided into three parts: landmark recognition part, needle insertion part, and connecting part, which are shown in blue, red, and light yellow, respectively (B). Two parts recognizing the sternal end of the clavicle and the costal arch were included in the novel design, and are shown in purple and orange (C). After the completion of the design, the whole navigational template was printed using stereolithography from photopolymer material (D).
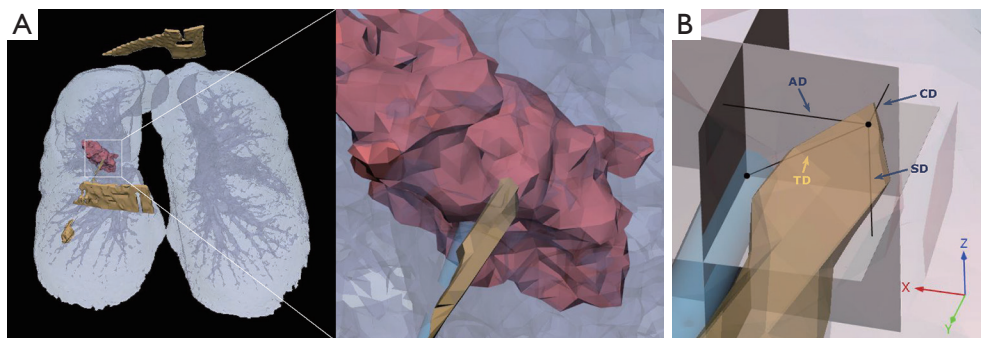

Figure S2 Deviation calculation method. The digital model of the lung (purple part), the lesion (red part), the designed insertion route (blue cylinder), and the real position of the template and biopsy needle (yellow part) was reconstructed (A). A rectangular coordinate system was established with the origin of the end of the designed route. AD, CD, and SD were measured separately, and TD was then calculated (B). AD, axial deviation; CD, coronal deviation; SD, sagittal deviation; TD, total deviation.
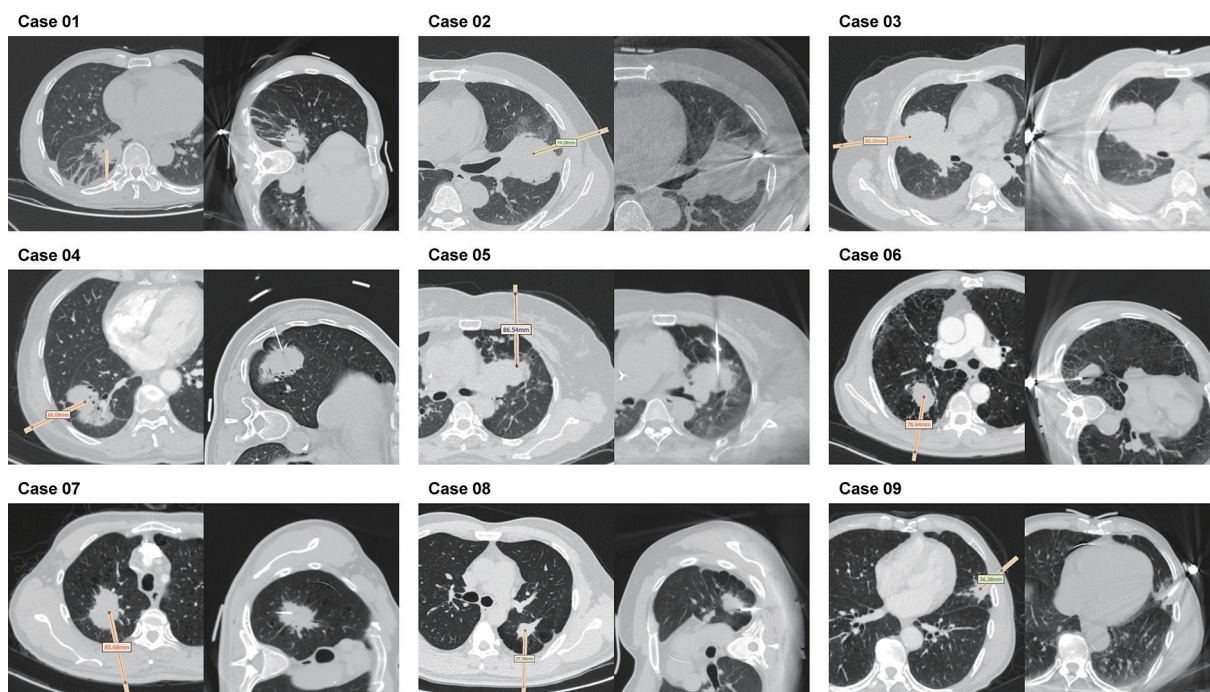
Figure S3 CT images of the 17 successful cases (Figures S3,S4). All the successful cases are presented according to the recruitment order. The CT images of insertion route design and real needle insertion were compared in every case. Cases 1 to 9 are included in this figure. CT, computed tomography.

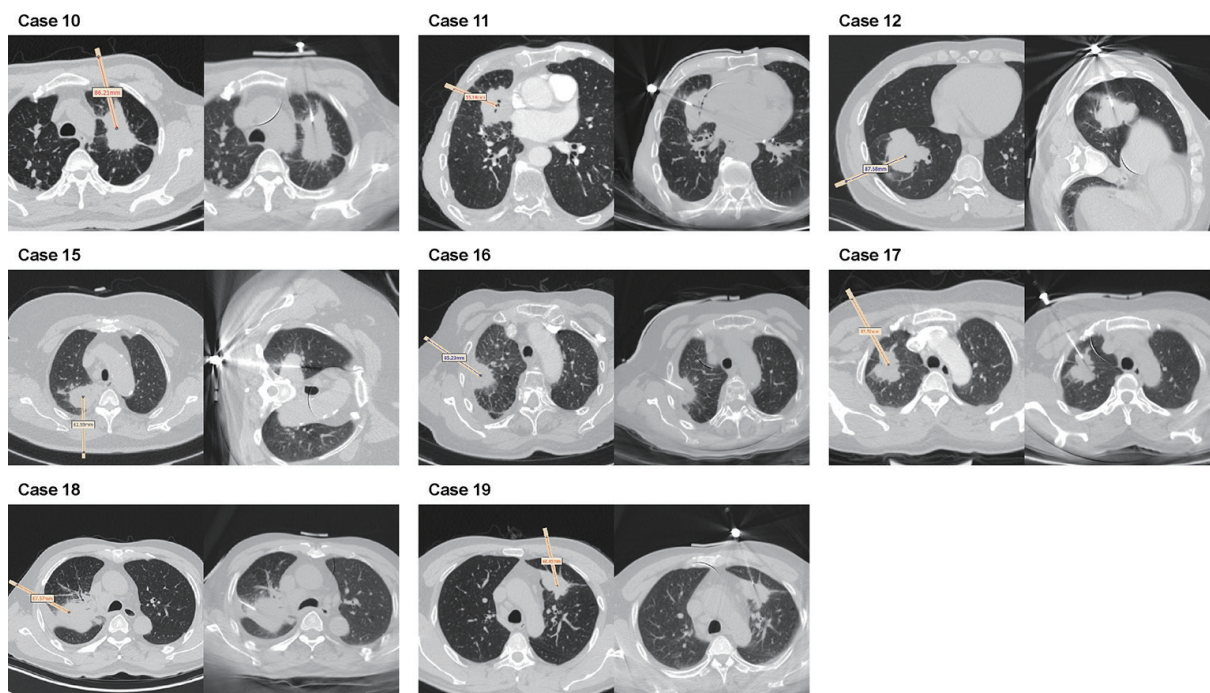**Figure S4** CT images of the 17 successful cases (Figures S3,S4). The CT images of insertion route design and real needle insertion of the other 8 successful cases are presented. Cases 13 and 20 were 2 patients who dropped out during the study, and case 14 was the case of template-guided biopsy failure. Hence, the CT images of these 3 cases are not shown in the figure. CT, computed tomography.
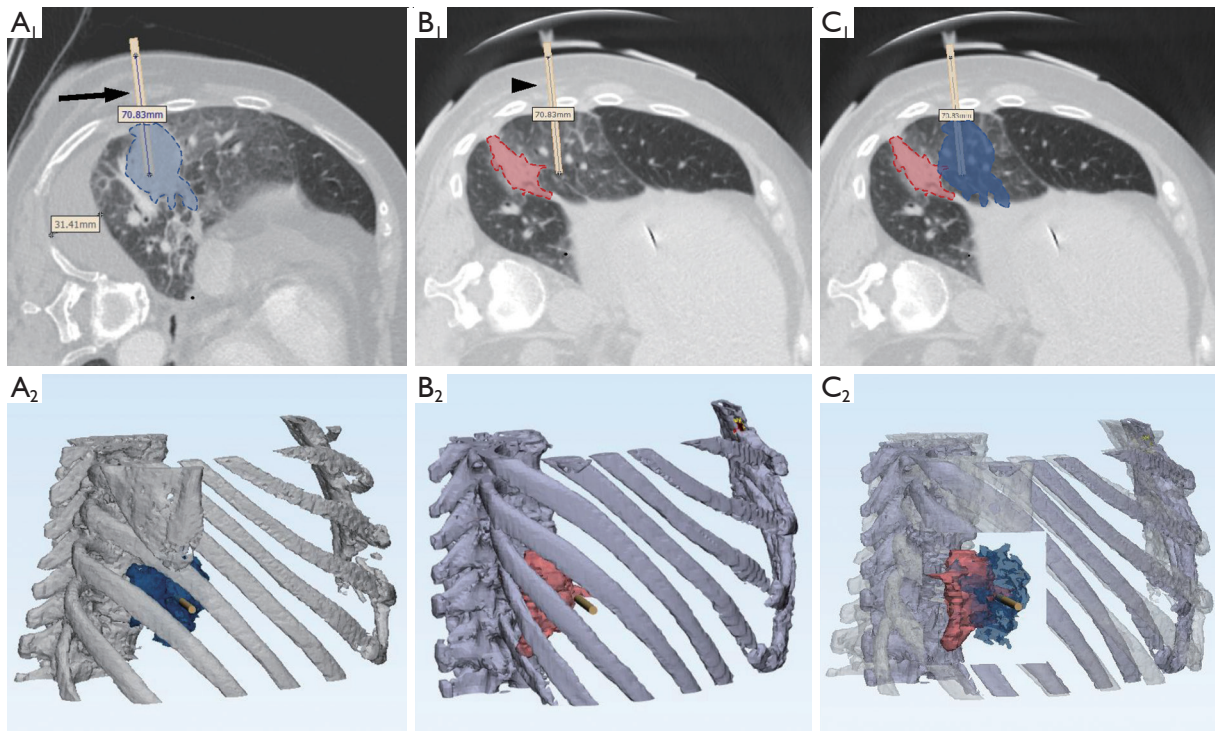
Figure S5 A failed case of template-guided FNA. The pre-biopsy CT image revealed a pleural effusion which measured 31.4 mm in the long-axis diameter in the right thoracic cavity (A1, the CT image is rotated 90° clockwise, and the blue part represents the target lesion). The designed insertion route (pointed by a black arrow) was through the right eighth intercostal space (A2, the route is indicated by a cylinder). When the participant adopted the lateral decubitus position for biopsy, the relative position between the thoracic cage and the lesion (red part) altered (B1,B2). The lesion could not be targeted through the predesigned route (pointed by a black arrowhead). The alteration of the lesion's position is clearly shown in the CT image and the reconstructed model (C1,C2). FNA, fine-needle aspiration; CT, computed tomography.

Table S1 Specific clinical characteristics of the 17 successful cases

Enrollment number	Sex	Age, years	BMI, kg/m^2	Nodule size, mm	Distance between lesion and pleura, mm	Nodule location	Biopsy type	Decubitus position	Length of the insertion route, mm
1	Male	66	20.20	39.3	11.2	RLL	FNA + CNB	Lateral	78.1
2	Male	61	25.71	56.0	0.0	LUL	FNA	Supine	74.3
3	Female	67	23.73	66.3	0.0	RML	FNA + CNB	Supine	82.3
4	Female	62	20.23	52.6	5.3	RLL	FNA	Lateral	66.1
5	Female	58	24.67	45.5	9.4	LUL	FNA + CNB	Supine	86.5
6	Male	70	22.76	38.3	16.6	RUL	FNA + CNB	Lateral	76.6
7	Male	64	19.59	45.5	4.4	RUL	FNA	Lateral	85.7
8	Male	37	25.91	32.4	5.3	LUL	FNA + CNB	Lateral	77.8
9	Male	72	21.08	31.7	0.0	LUL	FNA + CNB	Supine	36.4
10	Male	52	23.18	51.7	0.0	LUL	FNA	Supine	86.2
11	Male	74	17.81	41.4	15.9	RML	FNA	Supine	55.2
12	Male	45	27.73	52.5	11.4	RLL	FNA + CNB	Lateral	87.7
15	Female	65	29.69	41.0	0.0	RUL	FNA	Lateral	82.6
16	Female	75	24.98	33.4	0.0	RUL	FNA	Supine	85.2
17	Female	44	23.92	36.6	0.0	RUL	FNA	Supine	83.5
18	Male	59	20.96	44.2	0.0	RUL	FNA	Supine	87.6
19	Male	46	25.95	34.8	13.9	LUL	FNA	Supine	69.0

BMI, body mass index; RLL, right lower lobe; LUL, left upper lobe; RML, right middle lobe; RUL, right upper lobe; FNA, fine-needle aspiration; CNB, core needle biopsy.

Table S2 Specific clinicopathological information of the 17 successful cases

Enrollment number	Insertion deviation, mm				Procedural duration, min	DLP, mGy×cm	Complication	Cytological examination result
	CD	AD	SD	TD				
1	13.02	7.69	1.26	15.17	11.8	223.5	PNX	Adenocarcinoma
2	6.67	0.28	1.12	6.77	10.6	218.7	None	Poorly differentiated
3	0.86	5.42	3.12	6.31	10.8	249.3	None	Adenocarcinoma
4	1.07	7.24	5.94	9.43	11.9	187.1	None	Adenocarcinoma
5	1.34	6.71	0.52	6.86	10.7	179.6	None	Non-small cell carcinoma
6	0.11	10.65	0.35	10.66	9.7	173.0	None	Poorly differentiated
7	6.39	3.86	9.24	11.88	11.8	195.6	None	Non-small cell carcinoma
8	5.28	4.44	12.45	14.23	10.4	249.6	None	Inadequate sample
9	0.44	0.60	7.77	7.81	7.8	232.0	Pulm. Hem.	Suspicious for malignancy
10	2.10	2.48	4.25	5.35	11.3	201.5	Pulm. Hem.	Non-small cell carcinoma
11	1.53	2.29	9.45	9.84	9.7	256.0	None	Inadequate sample
12	3.72	2.43	11.88	12.68	7.1	207.1	PNX	Non-small cell carcinoma
15	6.30	8.00	1.50	10.29	13.3	231.0	None	Inadequate sample
16	0.63	9.21	6.78	11.45	6.4	220.9	None	Adenocarcinoma
17	0.53	7.35	2.61	7.82	9.7	211.4	None	Adenocarcinoma
18	3.05	1.51	3.20	4.67	11.6	253.4	Pulm. Hem.	Adenocarcinoma
19	4.75	0.06	5.92	7.59	13.5	288.6	None	Non-small cell carcinoma

CD, coronal deviation; AD, axial deviation; SD, sagittal deviation; TD, total deviation; DLP, dose-length product; PNX, pneumothorax; Pulm. Hem., pulmonary hemorrhage.
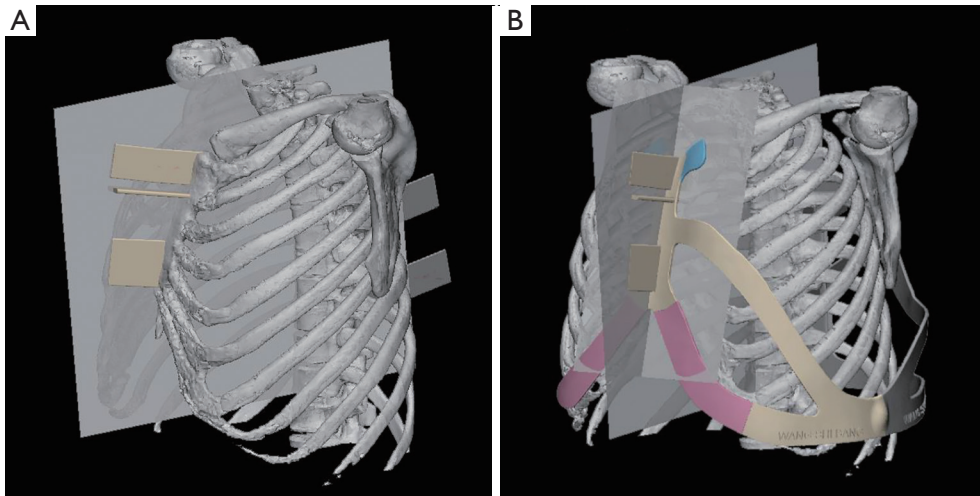
Figure S6 Indications of the newly-selected landmarks. The routinely chosen skeletal landmarks lay approximately in the same sagittal plane (A). Additional parts recognizing the sternal end of the clavicle (blue part) and the costal arch (red part) were added to the design of the template for reconfirming the position in the coronal plane (B).